

Article

# uPAR PET/CT for Prognostication and Response Assessment in Patients with Metastatic Castration-Resistant Prostate Cancer Undergoing Radium-223 Therapy: A Prospective Phase II Study

Marie Øbro Fosbøl<sup>1,2</sup>, Jann Mortensen<sup>1,2</sup>, Peter Meidahl Petersen<sup>3</sup>, Annika Loft<sup>1,2</sup>, Jacob Madsen<sup>1,2</sup> and Andreas Kjaer<sup>1,2,\*</sup>

- <sup>1</sup> Department of Clinical Physiology, Nuclear Medicine & PET, Copenhagen University Hospital, Rigshospitalet, 2100 Copenhagen, Denmark; marie.oebro.fosboel@regionh.dk (M.Ø.F.); jann.mortensen@regionh.dk (J.M.); annika.loft.jakobsen@regionh.dk (A.L.); jacob.madsen@regionh.dk (J.M.)
- <sup>2</sup> Cluster for Molecular Imaging, Department of Biomedical Sciences and Department of Clinical Medicine, University of Copenhagen, 2200 Copenhagen, Denmark
- <sup>3</sup> Department of Oncology, Copenhagen University Hospital, Rigshospitalet, 2100 Copenhagen, Denmark; peter.meidahl.petersen@regionh.dk
- \* Correspondence: akjaer@sund.ku.dk

**Citation:** Fosbøl, M.Ø.; Mortensen, J.; Petersen, P.M.; Loft, A.; Madsen, J.; Kjaer, A. uPAR PET/CT for Prognostication and Response Assessment in Patients with Metastatic Castration-Resistant Prostate Cancer Undergoing Radium-223 Therapy: A Prospective Phase II Study. *Diagnostics* **2021**, *11*, 1087. <https://doi.org/10.3390/diagnostics11061087>

Academic Editor: Alexander Haug

Received: 8 May 2021

Accepted: 8 June 2021

Published: 14 June 2021

**Publisher's Note:** MDPI stays neutral with regard to jurisdictional claims in published maps and institutional affiliations.



**Copyright:** © 2021 by the authors. Licensee MDPI, Basel, Switzerland. This article is an open access article distributed under the terms and conditions of the Creative Commons Attribution (CC BY) license (<http://creativecommons.org/licenses/by/4.0/>).

**Abstract:** The aim of this Phase II study was to investigate the potential for response assessment and prognostication of positron emission tomography (PET) using the ligand <sup>68</sup>Ga-NOTA-AE105 targeting the urokinase-type plasminogen activator receptor (uPAR) in patients receiving Radium-223-dichloride therapy (<sup>223</sup>RaCl<sub>2</sub>). A combined whole-body uPAR PET and computed tomography (CT) was performed before initiation of <sup>223</sup>RaCl<sub>2</sub> and after two cycles of therapy. Standardized uptake value (SUV) in selected bone metastases was measured and the lesion with the highest SUV<sub>max</sub> was considered the index lesion. Clinical outcomes were overall survival (OS), radiographic progression free survival (rPFS) and occurrence of symptomatic skeletal event (SSE). A total of 17 patients were included and 14 patients completed both baseline and follow-up uPAR-PET/CT. Baseline SUV<sub>max</sub> of the index lesion was associated with OS; hazard ratio 2.51 (95% CI: 1.01–6.28, *p* = 0.05) per unit increase in SUV<sub>max</sub>. No association between changes in SUV<sub>max</sub> from baseline to follow-up and OS, progression during therapy, or rPFS was found. Baseline SUV<sub>max</sub> was a significant predictor of SSE with receiver operating characteristics (ROC) area under the curve (AUC) = 0.81 (95% CI: 0.58–1.00, *p* = 0.034). A cut-off for tumor SUV<sub>max</sub> could be established with an odds ratio of 14.0 (95% CI: 1.14–172.6, *p* = 0.023) for occurrence of SSE within 12 months. Although based on a small number of patients, uPAR-PET SUV<sub>max</sub> in bone metastases was predictive for OS and risk of SSE in mCRPC patients receiving <sup>223</sup>RaCl<sub>2</sub>. However, a relatively low uptake of the uPAR ligand in bone metastases impedes visual evaluation and requires another modality for lesion delineation.

**Keywords:** urokinase-type plasminogen activator receptor (uPAR); prostate cancer; PET; Radium-223 therapy

## 1. Introduction

Radium-223-dichloride (<sup>223</sup>RaCl<sub>2</sub>) is the first alpha-emitting radionuclide therapy with a documented effect on overall survival (OS) and time to symptomatic skeletal related event (SSE) in patients with bone metastases from metastatic castration-resistant prostate cancer (mCRPC) [1,2]. However, interim response monitoring poses a clinical challenge. Dynamics of serum prostate specific antigen (PSA) is not an appropriate marker of response as only a minority of patients exhibit PSA decline during therapy [3]. Bone targeted imaging with either <sup>99m</sup>Tc-bisphosphonate bone scintigraphy or <sup>18</sup>F-fluoride

Positron emission tomography (PET) presents inherent limitations due to the “flare phenomenon”, making these modalities less suitable for timely assessment in therapy with  $^{223}\text{RaCl}_2$  [4].

A promising imaging target in this context is the urokinase-type plasminogen activator receptor (uPAR). uPAR is a cell membrane protein involved in regulating extracellular matrix proteolysis. In several types of malignant tumors and tumor-associated stromal cells, uPAR is overexpressed and high expression levels are associated with invasive potential, metastasis and resistance to chemotherapy [5–10]. The degree of uPAR expression in prostate cancer specimens is associated with important clinicopathological prognostic features, such as pathological tumor stage, Gleason score, positive surgical margins, and shorter biochemical recurrence free survival [11,12].

Quantification of uPAR expression could be a promising method of response assessment by estimating changes in the invasive potential of malignant tissue during the course of therapy. Non-invasive evaluation of uPAR expression is possible with the use of the uPAR specific PET imaging radioligand  $^{68}\text{Ga}$ -NOTA-AE105.  $^{68}\text{Ga}$ -NOTA-AE105 PET has been validated in a phase I study including prostate cancer patients, where uptake of the ligand corresponded to uPAR expression in excised tissue [13]. Additionally, in a recent phase II PET/MRI trial in patients with prostate cancer, we found a clear correlation between tumor uptake of the ligand and Gleason score, which confirmed the ligand as an imaging marker of prostate cancer aggressiveness [14].

We therefore hypothesized that  $^{68}\text{Ga}$ -NOTA-AE105 could offer a possibility for predicting the therapeutic effect of  $^{223}\text{RaCl}_2$  by evaluating early changes in uPAR expression during therapy. The objective of the current study was to evaluate the potential of uPAR PET/CT for interim response assessment among mCRPC patients treated with  $^{223}\text{RaCl}_2$ . A secondary aim was to explore the prognostic value of uPAR PET/CT in regard to overall survival (OS) and risk of SSE after therapy with  $^{223}\text{RaCl}_2$ .

## 2. Materials and Methods

### 2.1. Study Design

Between December 2016 and March 2018, patients who were referred for  $^{223}\text{RaCl}_2$  at our institution were screened for eligibility. Inclusion criteria were: mCRPC, planned therapy with  $^{223}\text{RaCl}_2$ , age  $\geq 18$  years and ability to give informed consent. Exclusion criteria were: Impaired communication skills or inability to understand study protocol, other known malignant disease or known allergy towards  $^{68}\text{Ga}$ -NOTA-AE105. Participants received  $^{223}\text{RaCl}_2$  therapy according to guidelines (55 kBq/kg intravenously every four weeks for up to six cycles). Clinical management of the patients was blinded for the uPAR PET results. Treatment was discontinued early in case of disease progression, unacceptable adverse events, declining performance status or by request from the patient. Patient characteristics collected at baseline included age, serum PSA, serum alkaline phosphatase, ECOG (Eastern Cooperative Oncology Group) performance status, and which systemic therapies for mCRPC the patients had received prior to  $^{223}\text{RaCl}_2$ .

The study protocol was approved by the Danish Medicines Agency (EudraCT no: 2016-002184-34; trial sponsor: Rigshospitalet) and the Regional Scientific Ethical Committee (Protocol no. H-16036551). Signature of written informed consent was obtained from all patients. The study was registered in ClinicalTrials.gov (NCT02964988) and was performed in accordance with the recommendation for good clinical practice (GCP) including independent monitoring by the GCP unit of the Capital Region of Denmark.

### 2.2. PET/CT Acquisition

uPAR PET/CT was conducted within 30 days prior to first cycle of  $^{223}\text{RaCl}_2$  and within 30 days after the second cycle of therapy. The PET/CT scans were performed using an integrated PET/CT system (Biograph64 mCT; Siemens Medical Solutions, Erlangen, Germany) starting 20 min after intravenous administration of a fixed dose of approximately

200 MBq  $^{68}\text{Ga}$ -NOTA-AE105. Synthesis of the ligand was performed as described earlier [13]. Whole-body PET scans from mid femur to vertex were obtained in 3-dimensional mode, with an acquisition time of 4 min per bed position. Attenuation and scatter corrected PET data were reconstructed iteratively using a 3D ordered subset expectation maximization (OSEM) with four iterations, eight subsets. A diagnostic CT with 2-mm slice thickness, 100 kV, and a quality reference of 265 mAs modulated by the Care Dose 4D automatic exposure control system (Siemens Medical Solutions, Erlangen, Germany) was performed before the PET-scan.

### 2.3. Image Analysis

PET/CT scans were evaluated by two board certified specialists in nuclear medicine blinded to clinical outcomes. Volumes of interest (VOIs) were drawn on baseline uPAR PET/CT images, corresponding to up to three bone metastases, in each participant. Selection of lesions was guided by baseline bone imaging (bone scintigraphy or  $^{18}\text{F}$ -fluoride PET), where the most prominent lesions were identified based on size and the level of tracer uptake. The same lesions were identified and delineated on follow-up uPAR PET/CT. Uptake of  $^{68}\text{Ga}$ -NOTA-AE105 in normal tissue for reference was measured by placing spheric VOIs in the right liver lobe, thoracic aorta and psoas muscle.

Uptake of the uPAR ligand in the VOIs was parameterized as maximum standardized uptake value ( $\text{SUV}_{\text{max}}$ ). For each participant, the lesion with the highest  $\text{SUV}_{\text{max}}$  at baseline, corresponding to the highest level of uPAR expression, was registered as the index lesion.

### 2.4. Clinical Outcomes

After inclusion, patients were followed from date of first uPAR PET/CT up to 18 months after or date of death. OS was defined as the time from first  $^{223}\text{RaCl}_2$  cycle to death of any cause. The occurrence of first SSE defined as new pathological symptomatic fracture, use of external beam radiation therapy (EBRT) for bone pain, and spinal cord compression or tumor-related orthopedic intervention was registered within 12 months from date of first  $^{223}\text{RaCl}_2$  cycle. Routine imaging for response assessment consisted of bone scintigraphy and CT of thorax and abdomen after three and six cycles of  $^{223}\text{RaCl}_2$ , respectively, performed by decision of the treating physician. Supplemental imaging procedures were performed in case of clinical suspicion of progression.

### 2.5. Statistical Analysis

Inter reader reliability of SUV-measurement was estimated using intraclass correlation coefficient (ICC). Kaplan–Meier statistics was used to calculate mean OS. Cox proportional hazards models were used to assess time-to-event outcomes: OS and radiographic progression free survival (rPFS) and association with  $\text{SUV}_{\text{max}}$ . Univariate logistic regression analysis was used to investigate association between  $\text{SUV}_{\text{max}}$  and progression during therapy. The association between occurrence of SSE and index lesion  $\text{SUV}_{\text{max}}$  as a continuous variable was investigated by receiver operating characteristics (ROC) analysis. Based on the ROC analysis, a cut-off value of  $\text{SUV}_{\text{max}}$  was identified to achieve the highest accuracy in prediction of SSE. Pearson's Chi-square test was used to calculate the odds ratio for the selected cutoff value in discriminating patients at risk of SSE.

Statistical analyses were performed in SPSS, version 25 (IBM Corp., Armonk, NY, USA). Cases with missing data were excluded listwise.  $p \leq 0.05$  was considered statistically significant.

## 3. Results

Seventeen patients were included in the study (Figure 1). According to the study protocol, 43 patients were originally planned to be included, but due to challenges in the recruitment of participants, in part due to a decreasing number of patients referred to

$^{223}\text{RaCl}_2$  treatment at our institution, the study was ended with a lower number of patients. Baseline characteristics are displayed in Table 1.

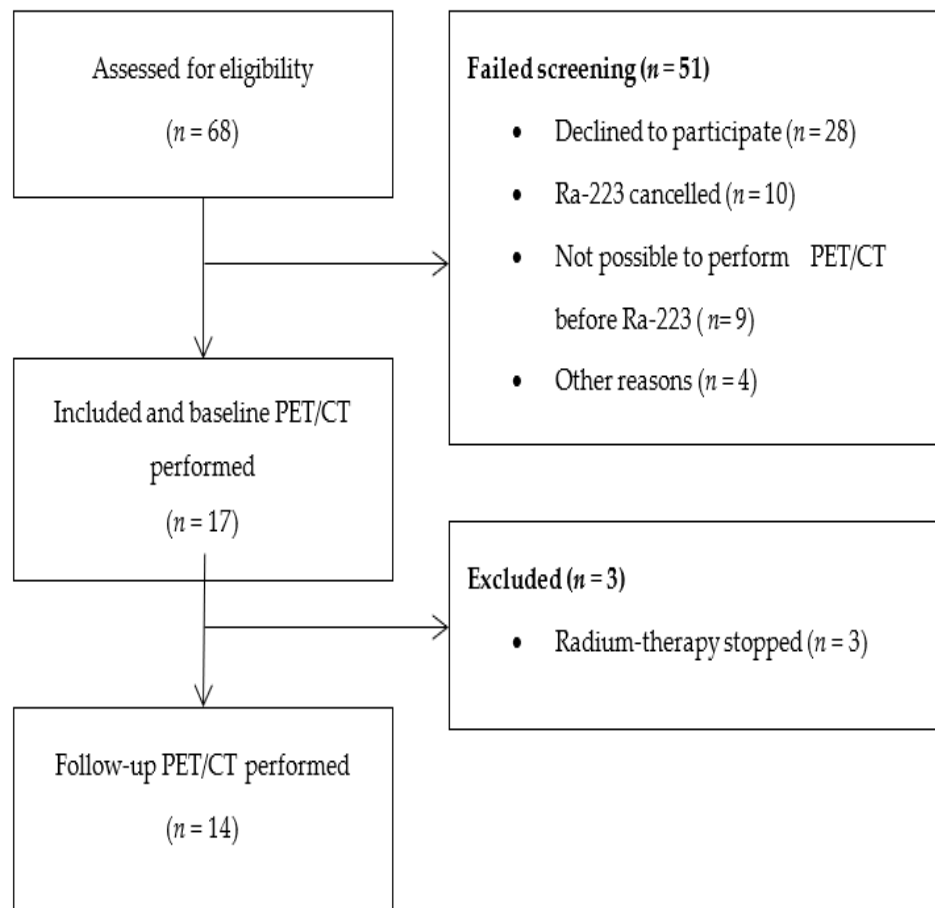


**Figure 1.** CONSORT diagram of the inclusion process.

Median time from baseline uPAR PET/CT to initiation of  $^{223}\text{RaCl}_2$  therapy was 4 days (range: 1–29). Patients received an intravenous dose of 200 MBq (median 201 MBq, range: 142–228 MBq)  $^{68}\text{Ga-NOTA-AE105}$  per PET scan. This activity corresponded to an effective dose of approximately 3.1 mSv per PET scan according to dosimetry calculations from the phase I trial [13]. No adverse events or reactions related to the administration were observed.

Three patients only received one cycle of  $^{223}\text{RaCl}_2$  and therefore did not undergo follow-up uPAR PET/CT. The reasons for discontinuation of therapy in these patients were deteriorating clinical condition (n = 2) and bone marrow suppression (n = 1). Median time from baseline uPAR PET/CT to follow-up scan was 56 days (range: 39–81 days).

**Table 1.** Patient characteristics at initiation of  $^{223}\text{RaCl}_2$ .

Pt. no.	Age (Years)	ECOG Performance Status	Number of Bone Metastases <sup>†</sup>	s-PSA ( $\mu\text{g/L}$ )	s-ALP <sup>†</sup> (U/L)	Previous Systemic Therapies for mCRPC
1	76	1	>20	931	NA	Doce, Caba, Enza, Abi
2	73	0	6–20	26	66	Doce
3	76	1	>20	7	82	Doce, Enza
4	78	1	>20	494	231	Doce, Caba, Enza, Abi
5	69	1	>20	318	99	Doce, Enza
6	81	1	6–20	109	73	Doce, Caba, Abi
7	63	0	<6	5	69	Doce
8	69	1	>20	235	271	Doce, Caba
9	76	1	>20	68	507	Doce, Caba
10	71	1	>20	52	350	Doce
11	82	0	>20	87	75	Enza, Abi
12	76	0	>20	119	85	Doce, Abi
13	78	1	>20	74	265	Doce, Enza
14	76	1	>20	942	108	Doce, Caba, Enza, Abi
15	79	1	>20	99	77	Enza, Abi
16	83	1	>20	77	98	Doce, Enza
17	77	1	6–20	113	140	Doce, Enza

PSA = Prostate specific antigen, ALP = Alkaline Phosphatase, Doce = Docetaxel, Caba = Cabazitaxel, Enza = Enzalutamide, Abi = Abiraterone. NA = Not assessed. <sup>†</sup> Number of bone metastases graded according to Soloway [15].

### 3.1. PET/CT Results

At baseline uPAR PET/CT a total of 46 metastatic lesions were delineated by each observer and 37 lesions at follow-up PET/CT. The interrater variability in terms of ICC was 0.75 (95% CI: 0.6–0.9) for lesions at baseline and 0.85 (95% CI: 0.71–0.92) at follow-up PET/CT.  $\text{SUV}_{\text{max}}$  of the index lesion (i.e., lesion with the highest  $\text{SUV}_{\text{max}}$ ) at baseline and follow-up for each participant is displayed in Table 2.

The mean  $\text{SUV}_{\text{max}}$  of all lesions for both observers was 2.10 (Range: 0.70–5.00) at baseline and 2.20 (Range: 0.82–4.00) at follow-up (examples in Figures 2 and 3). In normal liver tissue mean  $\text{SUV}_{\text{max}}$  was 1.87 (SD 0.40) at baseline and 1.88 (SD: 0.16) at follow-up. Mean  $\text{SUV}_{\text{max}}$  in the psoas muscle and thoracic aorta was 1.05 (SD 0.21)/1.17 (SD: 0.27) and 3.51 (SD: 0.60)/3.44 (SD: 0.41) at baseline/follow-up.

**Table 2.**  $^{68}\text{Ga}$ -NOTA-AE105 uptake in lesions and clinical outcomes. <sup>^</sup>  $\text{SUV}_{\text{max}}$  of the index lesion (mean of the two observers). \* Patients who completed < 2 cycles of  $^{223}\text{RaCl}_2$  did not undergo the follow-up uPAR PET/CT.

Pt. no.	$\text{SUV}_{\text{max}}$ <sup>^</sup> Baseline	$\text{SUV}_{\text{max}}$ <sup>^</sup> 2 Cycles	$\Delta\text{SUV}_{\text{max}}$	No. of $^{223}\text{Ra}$ Cycles	$\Delta\text{PSA}$ from Baseline to EOT (%)	$\Delta\text{ALP}$ from Baseline to EOT (%)	Radiographic Progression during Therapy	SSE (12 mo. from First $^{223}\text{Ra}$ )	OS (mo. from First $^{223}\text{Ra}$ )	Follow-Up (mo. from First $^{223}\text{Ra}$ )
1	3.92	NA *	NA *	1	NA	NA	NA	-	1.5	
2	2.09	1.65	-0.44	6	246.2	18.2	-	-		19.4
3	2.89	3.10	0.21	3	47.0	-23.2	Soft tissue	EBRT		18.9
4	1.90	NA *	NA *	1	NA	NA	Soft tissue	-	9.7	
5	2.53	2.45	-0.08	3	73.0	55.6	-	EBRT	14.2	
6	2.79	2.86	0.07	3	166.1	46.6	Bone	EBRT	11.5	
7	1.22	1.39	0.17	6	269.6	-13.0	-	-		20.2
8	2.11	2.55	0.44	5	86.0	21.0	Bone	-	7.3	
9	2.39	NA *	NA *	1	NA	NA	Soft tissue	Fracture	4.9	
10	2.79	2.92	0.13	4	73.1	-64.3	-	EBRT	16.7	
11	1.67	1.70	0.03	6	34.5	-60.0	-	-	17.1	
12	3.82	2.75	-1.07	3	106.7	-16.5	-	EBRT	7.7	
13	2.29	3.23	0.95	4	604.1	-30.9	-	-	12.0	
14	2.43	2.77	0.34	2	30.5	25.9	Soft tissue	-	2.5	

15	2.22	2.35	0.13	5	796.0	94.8	Bone + Soft tissue	Spinal cord compression	12.8
16	3.52	3.11	-0.41	3	10.8	28.6	Bone + Soft tissue	EBRT	6.2
17	2.59	2.93	0.35	6	252.2	-40.7	-	-	18.3

<sup>^</sup> SUV<sub>max</sub> of the index lesion (mean of the two observers). \* Patients who completed < 2 cycles of <sup>223</sup>RaCl<sub>2</sub> did not undergo the follow-up uPAR PET/CT.

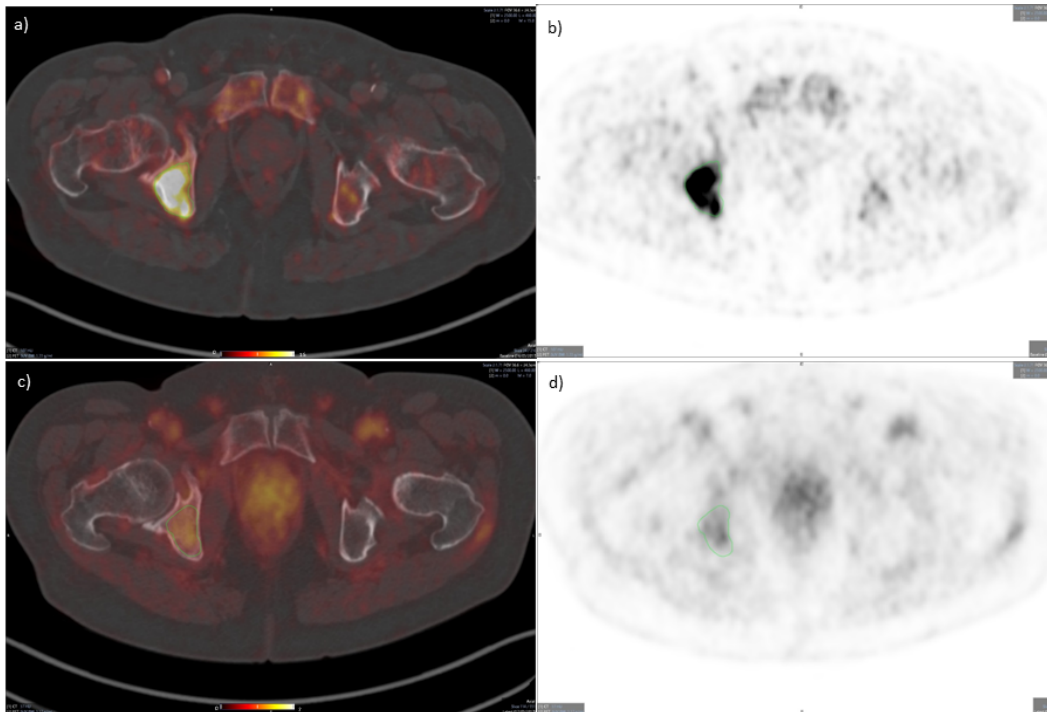


**Figure 2.** <sup>18</sup>F-fluoride and uPAR-PET/CT (patient 3) Transaxial fused images (left), PET images (right). a)+b): <sup>18</sup>F-fluoride PET/CT. c)+d): uPAR-PET/CT (bottom row). Bone metastasis in the pelvis is delineated. uPAR PET SUV<sub>max</sub> = 2.9.

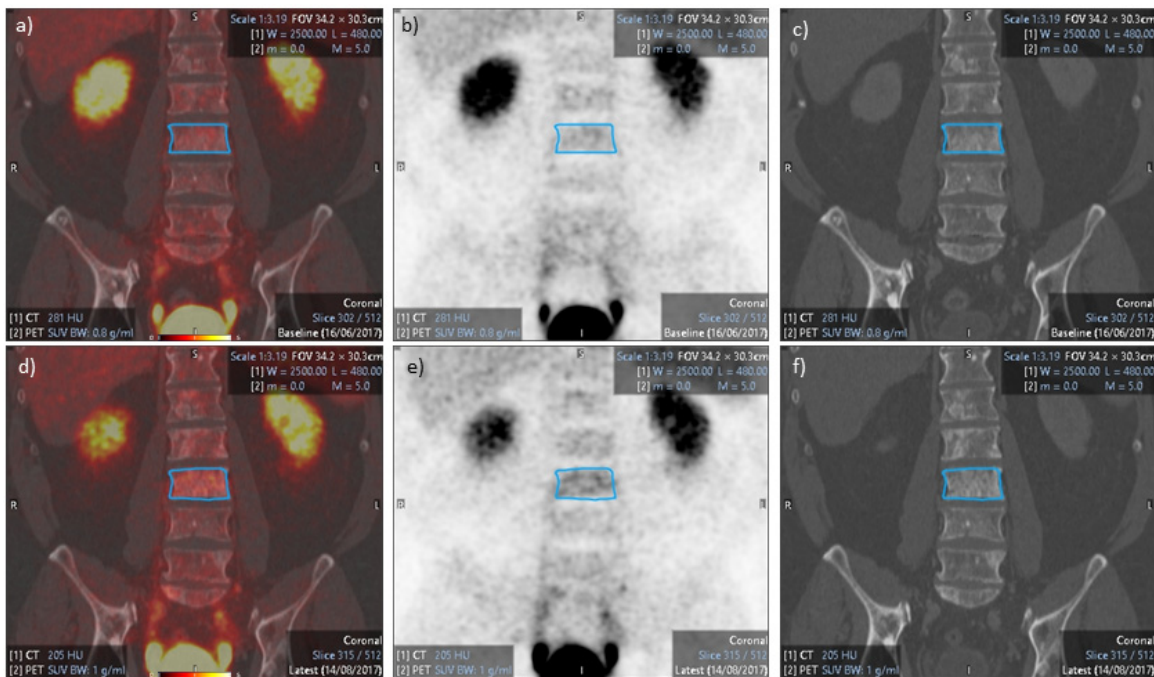


**Figure 3.** uPAR PET/CT (patient 10) Coronal fused images (left), PET images (centre) and CT images (right). Baseline images (a,b & c) and follow-up after two cycles of <sup>223</sup>RaCl<sub>2</sub> (d,e & f)). Bone metastasis in lumbar spine (L3) is delineated, baseline SUV<sub>max</sub> was 2.4 and after two cycles of <sup>223</sup>RaCl<sub>2</sub> increased to 3.9. After end of therapy the patient was diagnosed with epidural involvement at L3 and received EBRT to relieve symptoms.

### 3.2. Overall Survival

Mean OS was 11.9 months (95% CI: 9.1–14.8) from the first cycle of <sup>223</sup>RaCl<sub>2</sub>. For survival curve and median OS, please see Figure 4. There was a significant association between baseline SUV<sub>max</sub> of the index lesion and OS with a hazard ratio of 2.51 (95% CI: 1.01–6.28, *p* = 0.05) per unit increase in SUV<sub>max</sub>. Cox regression analysis for testing the association between mean SUV<sub>max</sub> of all lesions at baseline and OS only reached borderline statistical significance (Hazard ratio 3.36, 95% CI: 0.9–12.7, *p* = 0.07). No significant association between change in SUV<sub>max</sub> from baseline to follow-up and OS was found.

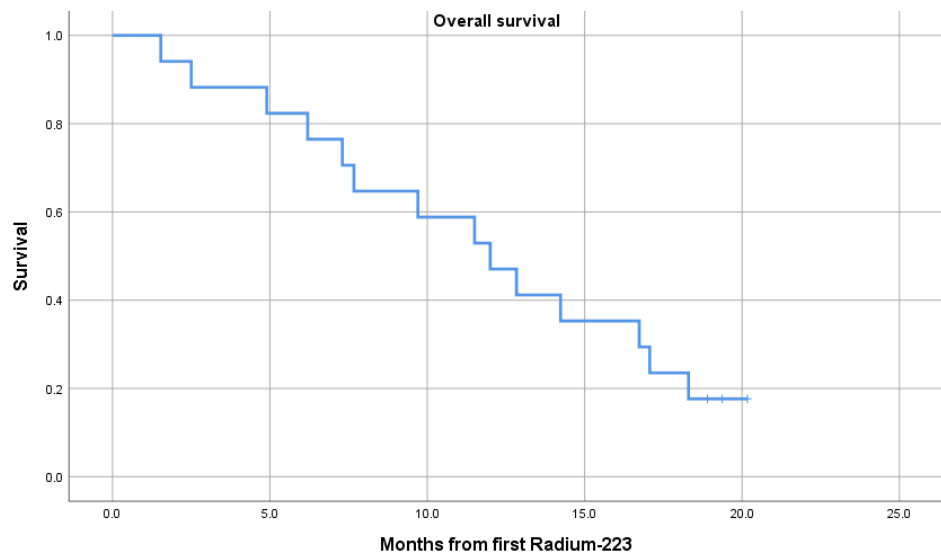


**Figure 4.** Kaplan-Meier curve of overall survival. Median OS 12 mo. (95% CI: 7.8–16.2).

### 3.3. Response

Eight patients (47%) experienced radiographic progression during therapy; four patients were diagnosed with progression in soft tissue, two patients with skeletal progression and two patients were classified as progressing in both bone and soft tissue. Median rPFS was 4.8 months (95% CI: 1.8–7.8). There was no significant association between SUV<sub>max</sub> of the index lesion (baseline value as well as change during therapy) and radiographic progression during therapy or rPFS.

### 3.4. Symptomatic Skeletal Events

During the first 12 months after initiation of <sup>223</sup>RaCl<sub>2</sub>-therapy, eight patients experienced a SSE (six patients with EBRT (35% of total), while there was one case of pathological symptomatic fracture (6%) and one patient with spinal cord compression (6%). ROC analysis of baseline SUV<sub>max</sub> of the index lesion as predictor of SSE had an area under the curve (AUC) = 0.81 (95% CI: 0.58–1.00, *p* = 0.034) (Figure 5). Based on the ROC analysis, a cutoff for obtaining the highest accuracy of SUV<sub>max</sub> = 2.34 was suggested. Patients with SUV<sub>max</sub> at baseline above this cutoff value had odds ratio = 14.0 (95% CI: 1.14–172.6, *p* = 0.023) for occurrence of SSE within 12 months. No significant association between changes in SUV<sub>max</sub> during therapy and the risk of SSE was found.

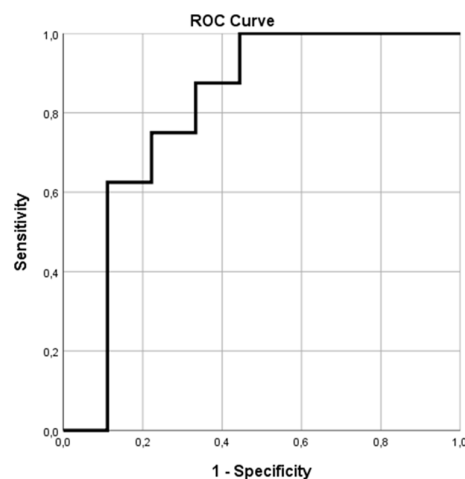


**Figure 5.** ROC curve analysis of SUV<sub>max</sub> of the index lesion in predicting occurrence of SSE. AUC = 0.81 (95% CI: 0.58–1.00, *p* = 0.034).

## 4. Discussion

Assessment of efficacy is important in all oncological treatments to avoid futile therapy with potential side-effects. In the case of <sup>223</sup>RaCl<sub>2</sub> therapy, there is no clear consensus regarding the role of imaging in the evaluation of interim response to therapy [16,17]. Although bone scintigraphy and <sup>18</sup>F-fluoride PET are the companion imaging agents of the bone targeted <sup>223</sup>RaCl<sub>2</sub> therapy, these modalities are not suitable for early response assessment. As increased osteoblastic activity in new and existing lesions can reflect effect of treatment as well as progression, response to <sup>223</sup>RaCl<sub>2</sub> cannot be evaluated before end of therapy [18]. This leads to a substantial risk that patients who do not benefit from <sup>223</sup>RaCl<sub>2</sub> therapy may continue ineffective treatment undetected.

In this phase II study, we wanted to assess whether uPAR PET/CT could serve as a method of early response assessment in patients with mCRPC treated with <sup>223</sup>RaCl<sub>2</sub>. We hypothesized that monitoring change in uPAR expression could provide an alternative approach to response assessment by imaging the invasive potential of the disease rather than bone remodeling. Although based on a small number of patients, SUV<sub>max</sub> at baseline

was significantly associated with survival and risk of SSE, thus indicating that the aggressiveness of prostate cancer lesions can be determined non-invasively by uPAR PET.

The small number of patients in the study was due to challenges in recruitment. As displayed in Table 1, the majority of participants had advanced disease with high PSA and extent of disease, which is representative of the patient cohort receiving  $^{223}\text{RaCl}_2$  at our institution. These patients are physically and mentally affected by their illness, and therefore more prone to decline participation in studies involving additional visits to the hospital. Furthermore, results from the ERA-223 trial [19], subsequent changes in guidelines regarding indication for  $^{223}\text{RaCl}_2$  therapy [20] as well as other emerging therapies for mCRPC becoming available, all led to a significant reduction in the number of patients eligible for inclusion. If it had been possible, more patients would have been advantageous to allow the addition of other variables in the prediction models and achieve more robust results.

Sensitivity in detection of metastases was not an endpoint of the study, and as the examples in Figures 2 and 3 show, the tumor-to-background ratio was not optimal for visualization of metastases. In fact, the selection of the bone lesions for quantitative analysis of uPAR ligand uptake was based upon bone scintigraphy. This represents a challenge in using uPAR PET/CT for staging or response assessment in mCRPC, especially in detection of new metastases. Additionally, the absolute changes in  $\text{SUV}_{\text{max}}$  in bone metastases after two cycles of  $^{223}\text{RaCl}_2$  were in most cases very discrete and were not associated with progression after end of therapy, which implies that uPAR PET should probably not be used for assessing response in this setting.

The reason for the relatively low uptake of uPAR ligand in bone metastases is yet to be determined. The binding peptide AE105 as well as the chelated form NOTA-AE105 are antagonists with high affinity for uPAR as validated in several studies [13,21–23]. Consequently, if the uPA/uPAR system was highly activated in the bone lesions, one might expect a more marked uptake. Nevertheless, the finding of this study of a clear association between avidity on uPAR PET and OS, strongly supports that uPAR PET does reflect the uPAR expression. However, in the present study, it was not possible to obtain biopsies from bone metastases to directly validate the expression of uPAR. It has been demonstrated that the uPA/uPAR system plays an important part in osseous metastatic dissemination in prostate cancer. Accordingly, blocking the uPAR signaling with either anti-uPAR antibody or antisense oligonucleotides reduced development of bone metastases in mice inoculated with prostate cancer cells [8,24]. Likewise, uPA-silenced prostate cancer cells inoculated in xenograft bone in mice exhibited decreased growth and tumor size [25]. Therefore, the relatively moderate uptake of  $^{68}\text{Ga}$ -NOTA-AE105 implies that, although the uPA/uPAR system is active in the formation of new bone lesions, the expression may shift and be lower in existing bone metastases.

The challenge of identifying metastases due to low tumor-to-background ratio can be circumvented by combining uPAR PET with anatomically detailed imaging as magnetic resonance imaging (MRI) or with bone scintigraphy (SPECT or PET).

Other imaging modalities for assessment of response to  $^{223}\text{RaCl}_2$  have been proposed [18]. An appealing option in this setting is  $^{68}\text{Ga}$ -PSMA PET/CT [26] which, as opposed to bone targeted imaging, can detect metastatic disease in both bone and soft tissue. Additionally, interim response assessment is not distorted by the flare phenomenon as seen with bone targeted imaging. Recently, a proposal for PSMA PET response assessment in systemic therapy has been published [27], but is yet to be validated prospectively.

## 5. Conclusions

In conclusion, this phase II study found that the non-invasive quantitative evaluation of uPAR expression by uPAR-PET using  $^{68}\text{Ga}$ -NOTA-AE105 can provide prognostic information regarding OS and risk of SSE in patients with advanced mCRPC receiving  $^{223}\text{RaCl}_2$ . A relatively low uptake of the uPAR ligand in bone metastasis impedes direct visual evaluation and requires another modality, e.g., bone scintigraphy or MRI, for lesion

delineation. The change in  $^{68}\text{Ga}$ -NOTA-AE105 uptake after two cycles of  $^{223}\text{RaCl}_2$  therapy was not associated with disease progression.

**Author Contributions:** Conceptualization, M.Ø.F. and A.K.; methodology, M.Ø.F., A.L., A.K., and J.M. (Jacob Madsen); validation, M.Ø.F. and A.L.; formal analysis, M.Ø.F. and A.L.; investigation, M.Ø.F. and A.L.; resources, J.M. (Jacob Madsen), A.L., P.M.P., J.M. (Jann Mortensen), and A.K.; data curation, M.Ø.F.; writing—original draft preparation, M.Ø.F.; writing—review and editing, M.Ø.F., J.M. (Jann Mortensen), P.M.P., A.L., J.M., and A.K.; visualization, M.Ø.F.; supervision, A.K., J.M. (Jann Mortensen), and P.M.P.; project administration, M.Ø.F.; funding acquisition, A.K. All authors have read and agreed to the published version of the manuscript.

**Funding:** This project received funding from the European Union’s Horizon 2020 research and innovation programme under grant agreements no. 670261 (ERC Advanced Grant) and 668532 (Click-It), the Lundbeck Foundation, the Novo Nordisk Foundation, the Innovation Fund Denmark, the Danish Cancer Society, Arvid Nilsson Foundation, Svend Andersen Foundation, the Neye Foundation, the Research Foundation of Rigshospitalet, the Danish National Research Foundation (grant 126), the Research Council of the Capital Region of Denmark, the Danish Health Authority, the John and Birthe Meyer Foundation and Research Council for Independent Research.

**Institutional Review Board Statement:** The study was conducted according to the guidelines of the Declaration of Helsinki, and approved by the Ethics Committee of Region Hovedstaden, Denmark (protocol code H-16036551 approved 10-10-2016) and the Danish Medicines Agency (EudraCT no: 2016-002184-34; trial sponsor: Rigshospitalet).

**Informed Consent Statement:** Informed consent was obtained from all subjects involved in the study.

**Data Availability Statement:** The data presented in this study are available on request from the corresponding author. The data are not publicly available due to restrictions by the Danish Agency for Data Protection.

**Conflicts of Interest:** Jacob Madsen (J.M.) and Andreas Kjaer (A.K.) are inventors on a filed patent application: Positron Emitting Radionuclides Labeled Peptides for Human uPAR PET Imaging (WO 2014086364 A1). J.M. and A.K. are cofounders of Curasight, which has acquired IPR for the uPAR PET technology to commercialize it. No other potential conflict of interest relevant to this article was reported.

## References

1. Parker, C.; Nilsson, D.S.; Heinrich, S.D.; Helle, S.I.; O’Sullivan, J.M.; Fosså, S.D.; Chodacki, A.; Wiechno, P.; Logue, J.; Seke, M.; et al. Alpha Emitter Radium-223 and Survival in Metastatic Prostate Cancer. *New Engl. J. Med.* **2013**, *369*, 213–223, doi:10.1056/nejmoa1213755.
2. Sartor, O.; Coleman, R.; Nilsson, S.; Heinrich, D.; Helle, S.; O’Sullivan, J.M.; Fosså, S.D.; Chodacki, A.; Wiechno, P.; Logue, J.; et al. Effect of radium-223 dichloride on symptomatic skeletal events in patients with castration-resistant prostate cancer and bone metastases: results from a phase 3, double-blind, randomised trial. *Lancet Oncol.* **2014**, *15*, 738–746, doi:10.1016/s1470-2045(14)70183-4.
3. Sartor, O.; Coleman, R.E.; Nilsson, S.; Heinrich, D.; Helle, S.I.; O’Sullivan, J.M.; Vogelzang, N.J.; Bruland, Ø.; Kobina, S.; Wilhelm, S.; et al. An exploratory analysis of alkaline phosphatase, lactate dehydrogenase, and prostate-specific antigen dynamics in the phase 3 ALSYMPCA trial with radium-223. *Ann. Oncol.* **2017**, *28*, 1090–1097, doi:10.1093/annonc/mdx044.
4. Isensee, G.; Péporté, A.; Müller, J.; Schmid, S.; Gillissen, S.; Omlin, A. Is There a Flare Phenomenon on Bone Scintigraphy in Men With Advanced Prostate Cancer Treated With Radium-223? *Clin. Genitourin. Cancer* **2018**, *16*, 349–354, doi:10.1016/j.clgc.2018.04.002.
5. Huang, Z.; Wang, L.; Wang, Y.; Zhuo, Y.; Li, H.; Chen, J.; Chen, W. Overexpression of CD147 contributes to the chemoresistance of head and neck squamous cell carcinoma cells. *J. Oral Pathol. Med.* **2013**, *42*, 541–546, doi:10.1111/jop.12046.
6. Wang, K.; Xing, Z.-H.; Jiang, Q.-W.; Yang, Y.; Huang, J.-R.; Yuan, M.-L.; Wei, M.-N.; Li, Y.; Wang, S.-T.; Liu, K.; et al. Targeting uPAR by CRISPR/Cas9 System Attenuates Cancer Malignancy and Multidrug Resistance. *Front. Oncol.* **2019**, *9*, 80, doi:10.3389/fonc.2019.00080.
7. Eastman, B.M.; Jo, M.; Webb, D.L.; Takimoto, S.; Gonias, S.L. A transformation in the mechanism by which the urokinase receptor signals provides a selection advantage for estrogen receptor-expressing breast cancer cells in the absence of estrogen. *Cell. Signal.* **2012**, *24*, 1847–1855, doi:10.1016/j.cellsig.2012.05.011.
8. Rabbani, S.A.; Ateeq, B.; Arakelian, A.; Valentino, M.L.; Shaw, D.E.; Dauffenbach, L.M.; Kerfoot, C.A.; Mazar, A.P. An Anti-Urokinase Plasminogen Activator Receptor Antibody (ATN-658) Blocks Prostate Cancer Invasion, Migration, Growth, and Experimental Skeletal Metastasis In Vitro and In Vivo. *Neoplasia* **2010**, *12*, 778–788, doi:10.1593/neo.10296.

9. Mahmood, N.; Mihalciou, C.; Rabhani, S.A. Multifaceted Role of the Urokinase-Type Plasminogen Activator (uPA) and Its Receptor (uPAR): Diagnostic, Prognostic, and Therapeutic Applications. *Front. Oncol.* **2018**, *8*, 24, doi:10.3389/fonc.2018.00024.
10. Smith, H.W. and Marshall, C.J. Regulation of cell signalling by uPAR. *Nat. Rev. Mol. Cell Biol.* **2010**, 23–36, doi: 10.1038/nrm2821.
11. Kumano, M.; Miyake, H.; Muramaki, M.; Furukawa, J.; Takenaka, A.; Fujisawa, M. Expression of urokinase-type plasminogen activator system in prostate cancer: Correlation with clinicopathological outcomes in patients undergoing radical prostatectomy. *Urol. Oncol. Semin. Orig. Investig.* **2009**, *27*, 180–186, doi:10.1016/j.urolonc.2008.01.012.
12. Cozzi, P.J.; Wang, J.; Delprado, W.; Madigan, M.C.; Fairy, S.; Russell, P.J.; Li, Y. Evaluation of urokinase plasminogen activator and its receptor in different grades of human prostate cancer☆. *Hum. Pathol.* **2006**, *37*, 1442–1451, doi:10.1016/j.humpath.2006.05.002.
13. Skovgaard, D.; Persson, M.; Brandt-Larsen, M.; Christensen, C.; Madsen, J.; Klausen, T.L.; Holm, S.; Andersen, F.L.; Loft, A.; Berthelsen, A.K.; et al. Safety, Dosimetry, and Tumor Detection Ability of 68 Ga-NOTA-AE105: First-in-Human Study of a Novel Radioligand for uPAR PET Imaging. *J. Nucl. Med.* **2017**, *58*, 379–386, doi:10.2967/jnumed.116.178970.
14. Fosbøl, M. Øbro; Kurbegovic, S.; Johannesen, H.H.; Røder, M.A.; Hansen, A.E.; Mortensen, J.; Loft, A.; Petersen, P.M.; Madsen, J.; Brasso, K.; et al. Urokinase-Type Plasminogen Activator Receptor (uPAR) PET/MRI of Prostate Cancer for Noninvasive Evaluation of Aggressiveness: Comparison with Gleason Score in a Prospective Phase 2 Clinical Trial. *J. Nucl. Med.* **2021**, *62*, 354–359, doi:10.2967/jnumed.120.248120.
15. Soloway, M.S.; Hardeman, S.W.; Hickey, D.; Todd, B.; Soloway, S.; Raymond, J.; Moinuddin, M. Stratification of patients with metastatic prostate cancer based on extent of disease on initial bone scan. *Cancer* **1988**, *61*, 195–202, doi:10.1002/1097-0142(19880101)61:13.co;2-y.
16. Heinrich, D.; Bektic, J.; Bergman, A.M.; Caffo, O.; Cathomas, R.; Chi, K.N.; Daugaard, G.; Keizman, D.; Kindblom, J.; Kramer, G.; et al. The Contemporary Use of Radium-223 in Metastatic Castration-resistant Prostate Cancer. *Clin. Genitourin. Cancer* **2018**, *16*, e223–e231, doi:10.1016/j.clgc.2017.08.020.
17. Parker, C.; Heidenreich, A.; Nilsson, S.; Shore, N. Current approaches to incorporation of radium-223 in clinical practice. *Prostate Cancer Prostatic Dis.* **2018**, *21*, 37–47, doi:10.1038/s41391-017-0020-y.
18. Etchebehere, E.; Brito, A.E.; Rezaee, A.; Langsteger, W.; Beheshti, M. Therapy assessment of bone metastatic disease in the era of 223radium. *Eur. J. Nucl. Med. Mol. Imaging* **2017**, *44*, 84–96, doi:10.1007/s00259-017-3734-0.
19. Smith, M.; Parker, C.; Saad, F.; Miller, K.; Tombal, B.; Ng, Q.S.; Boegemann, M.; Matveev, V.; Piulats, J.M.; Zucca, L.E.; et al. Addition of radium-223 to abiraterone acetate and prednisone or prednisolone in patients with castration-resistant prostate cancer and bone metastases (ERA 223): a randomised, double-blind, placebo-controlled, phase 3 trial. *Lancet Oncol.* **2019**, *20*, 408–419, doi:10.1016/s1470-2045(18)30860-x.
20. Mottet, N.; van den Bergh, R.C.N.; Briers, E.; van den Broeck, T.; Cumberbatch, M.G.; De Santis, M.; Fanti, S.; Fossati, N.; Gandaglia, G.; Gillesen, S.; Grivas, N., et al. EAU Guidelines. Edn. presented at the EAU Annual Congress Barcelona 2019, **2019**. <http://uroweb.org/guidelines/compilations-of-all-guidelines/>. Accessed April 26 2021.
21. Persson, M.; Hosseini, M.; Madsen, J.; Jørgensen, T.J.D.; Jensen, K.J.; Kjaer, A.; Ploug, M. Improved PET Imaging of uPAR Expression Using new 64Cu-labeled Cross-Bridged Peptide Ligands: Comparative in vitro and in vivo Studies. *Theranostics* **2013**, *3*, 618–632, doi:10.7150/thno.6810.
22. Persson, M.; Madsen, J.; Østergaard, S.; Jensen, M.M.; Jørgensen, J.T.; Juhl, K.; Lehmann, C.; Ploug, M.; Kjaer, A. Quantitative PET of Human Urokinase-Type Plasminogen Activator Receptor with 64Cu-DOTA-AE105: Implications for Visualizing Cancer Invasion. *J. Nucl. Med.* **2012**, *53*, 138–145, doi:10.2967/jnumed.110.083386.
23. Persson, M.; Madsen, J.; Østergaard, S.; Ploug, M.; Kjaer, A. 68Ga-labeling and in vivo evaluation of a uPAR binding DOTA- and NODAGA-conjugated peptide for PET imaging of invasive cancers. *Nucl. Med. Biol.* **2012**, *39*, 560–569, doi:10.1016/j.nucmed-bio.2011.10.011.
24. Margheri, F.; D'Alessio, S.; Serrati, S.; Pucci, M.; Annunziato, F.; Cosmi, L.; Liotta, F.; Angeli, R.; Angelucci, A.; Gravina, G.L.; et al. Effects of blocking urokinase receptor signaling by antisense oligonucleotides in a mouse model of experimental prostate cancer bone metastases. *Gene Ther.* **2005**, *12*, 702–714, doi:10.1038/sj.gt.3302456.
25. Dong, Z.; Saliganan, A.D.; Meng, H.; Nabha, S.M.; Sabbota, A.L.; Sheng, S.; Bonfil, R.D.; Cher, M.L. Prostate Cancer Cell-Derived Urokinase-Type Plasminogen Activator Contributes to Intraosseous Tumor Growth and Bone Turnover. *Neoplasia* **2008**, *10*, 439–449, doi:10.1593/neo.08106.
26. Uprimny, C.; Kroiss, A.; Nilica, B.; Buxbaum, S.; Decristoforo, C.; Horninger, W.; Virgolini, I.J. 68Ga-PSMA ligand PET versus 18F-NaF PET: evaluation of response to 223Ra therapy in a prostate cancer patient. *Eur. J. Nucl. Med. Mol. Imaging* **2015**, *42*, 362–363, doi:10.1007/s00259-014-2922-4.
27. Fanti, S.; Hadaschik, B.; Herrmann, K. Proposal for Systemic-Therapy Response-Assessment Criteria at the Time of PSMA PET/CT Imaging: The PSMA PET Progression Criteria. *J. Nucl. Med.* **2019**, *61*, 678–682, doi:10.2967/jnumed.119.233817.